Chapter 13

Ambient Level of NO_x and NO_y as Indicators of Photochemical Activity in an Urban Center

Alberto Mendoza and Edson R. Carrillo

Additional information is available at the end of the chapter

http://dx.doi.org/10.5772/59752

1. Introduction

Atmospheric pollution is considered a severe problem, especially in large urban areas where anthropogenic emissions (e.g., emissions from domestic, industrial, and transportation activities, as well as from other productive sectors) mix with biogenic emissions (i.e., emissions with natural origins). Anthropogenic emissions include gas-phase primary air pollutants such as nitric oxide (NO), nitrogen dioxide (NO_2), carbon monoxide (CO), volatile organic compounds (VOCs), and sulfur dioxide (SO_2). Although these pollutants can produce harmful health effects, their ability to react as precursors of secondary air pollutants is one of their most relevant characteristics.

Ozone (O_3) is produced as a secondary pollutant by photochemical reactions occurring between nitrogen oxides (NO_x, where $NO_x = NO + NO_2$) and VOCs in the presence of sunlight [1, 2]. For a long time, interest in O_3 focused on its direct health effects as a major constituent of photochemical air pollution [3, 4] and its impacts on vegetation [5, 6]. However, O_3 also affects the energy budget of the atmosphere; thus, it has become part of a family of species referred to as short-lived climate pollutants (SLCP) [7].

Photochemical activity occurs in both natural and human-altered environments. Theoretically, in the presence of only NO_x in the troposphere, O_3 generation could be described by a simple mechanism known as the NO_x-O_3 photostationary state, summarized by the following reactions:

$$NO_2 + h\nu \rightarrow NO + O_3 \quad (1)$$

$$O^{\bullet} + O_2 + M \rightarrow O_3 + M \tag{2}$$

$$O_3 + NO \rightarrow NO_2 + O_2, \tag{3}$$

where *hv* represents a photon (sunlight energy), $O^{\bullet}$ denotes an oxygen free radical (an oxygen atom with an unpaired electron), and *M* is known as a third body (molecule) that acts as an energy sink. In the atmosphere, this third body is typically N_2 or O_2. Under this chemical reaction scheme, the net O_3 production is zero, and according to the photostationary state equation, the concentration of O_3 can be determined based on the concentration of NO_x and the amount of solar radiation:

$$\left[O_3\right]_{ps} = \left(\frac{j_{NO_2}}{k_{R3}}\right)\frac{\left[NO_2\right]}{\left[NO\right]}, \tag{4}$$

where k_{R3} is the kinetic reaction rate constant for reaction (3) and j_{NO2} is the photolysis rate of NO_2. As a demonstration, if a 10 parts per billion (ppb) value is considered for the term j_{NO2}/k_{R3}, the O_3 concentration would be 27 ppb, with an initial value of 100 ppb of NO [8]. An O_3 concentration ranging between 10–40 ppb is typical of rural areas around the globe [9].

When VOCs are added to the mixture of species present in the troposphere, the observed O_3 levels are higher than those predicted by the photostationary state formulation. In this case, interactions in the O_3-NO_x-VOC system are initialized by the hydroxyl ($HO^{\bullet}$) radical, through the photolysis of O_3:

$$O_3 + hv \rightarrow O_2 + O\left(^1D\right) \tag{5}$$

$$O\left(^1D\right) + H_2O \rightarrow 2HO^{\bullet}, \tag{6}$$

where $O(^1D)$ represents an excited singlet oxygen atom. The oxidation of the VOCs (represented here as RH, where R is an organic functional group, e.g., an alkyl group) continues in the presence of $HO^{\bullet}$ and NO_x to produce more O_3 and a variety of nitrogen-containing species. The process can be represented by the following generalized reactions [8]:

$$RH + HO^{\bullet} + O_2 \rightarrow RO_2^{\bullet} + H_2O. \tag{7}$$

The alkyl peroxide radical ($RO_2^{\bullet}$) reacts with NO to form aldehydes (R'CHO) and peroxide radicals ($HO_2^{\bullet}$):

http://dx.doi.org/10.5772/59752

$$RO_2^{\bullet} + NO + O_2 \rightarrow NO_2 + R'CHO + HO_2^{\bullet} \quad (8)$$

Reaction 8 is a relevant process because it represents an alternate route for the production of NO_2 from NO, but without destroying O_3 (in contrast to reaction [3]). A similar process occurs when the aldehydes continue reacting to eventually form acyl peroxy radicals ($R'C(O)O_2^{\bullet}$) that undergo a similar fate as the $RO_2^{\bullet}$ radicals in reaction (8). Thus, O_3 starts to accumulate in the system, as it is no longer destroyed by reaction (3). It continues to be produced by reactions (1) and (2) as NO_2 and NO cycle through this set of reactions. In addition, the $RO_2^{\bullet}$ radicals can produce nitrates when they react with NO_2:

$$RO_2^{\bullet} + NO + M \rightarrow RONO_2 + M \quad (9)$$

$$HO^{\bullet} + NO_2 + M \rightarrow HNO_3 + M. \quad (10)$$

This description is not exhaustive, as we have focused our attention on the main reactions of O_3 production by NO_x and VOCs. As indicated, NO_x acts as catalyst in these reactions, while the VOCs continue to undergo oxidation until they are converted to CO_2. In parallel, a variety of different inorganic (e.g., HNO_3) and organic (e.g., $RONO_2$) nitrogen-containing species are also produced. Some of these substances act as reservoirs of NO_x which are released to the reacting mixture upon decomposition (e.g., peroxy acetyl nitrate or PAN, an organic nitrate), and others act as sinks (most notably, HNO_3). The sum of NO_x and these additional inorganic and organic nitrates is referred to as total reactive nitrogen or total odd nitrogen oxides (NO_y).

In general, the O_3-NO_x-VOC system increases the NO_x available to react through reactions (1)-(2) (increasing O_3), thereby producing a complex mixture of partially oxidized VOCs that mixes with freshly emitted VOCs and different oxidized nitrogen species (HNO_3, HNO_2, NO_3, PAN, etc.). The study of the dynamics of O_3 production can be quite challenging, given the complexity of the chemical mixtures and their nonlinear response to emission changes and meteorological conditions. For this reason, comprehensive air quality models have been devised to study the complex physical and chemical processes that participate in gas-phase production of O_3 and other air pollutants [10].

Observational-based approaches have proven to be valuable for describing the conditions and regimes that foster air pollution. Some observational approaches use considerable amounts of data that can be obtained through networks of routine air quality and meteorological monitoring stations, and conclusions are then inferred based on the statistical analysis of these data [11-17]. The analyses of these databases can be enhanced if information is also available for additional indicator species that are typically not routinely monitored, such as NO_y.

In this study, we have analyzed data gathered by the routine air quality monitoring stations of the Monterrey Metropolitan Area (MMA; 25° 40′ N, 100° 18′ W). Monterrey is the third most populated urban center in Mexico (4.1 million inhabitants), second in size in the country in

terms of industrial infrastructure, and one of the cities with the worst air quality problems in Mexico [18]. The MMA (see Figure 1) has been in violation of the 1-hr Mexican Air Quality Standard for O_3 (0.11 ppm) since the establishment of its routine air quality monitoring system in 1993. For example, the 1-hr O_3 standard was exceeded on 48 different days in 2011 [19]. Peak O_3 concentrations can reach 170 ppb and typically occur at the downtown or western air quality stations [20]. Some studies report that the MMA is the fifth most polluted Latin American city in terms of O_3 [21]. In addition to the large number of industrial facilities located inside or nearby the metropolitan area that contribute to the poor air quality, emissions from several gas-fired electric utilities and one of the six refineries that operate in the country (located less than 40 km to the east of downtown Monterrey) add to the anthropogenic burden imposed on the airshed. Despite the importance of the contribution of area and point sources to the total emissions inventory, the mobile sources represent approximately 75% of the total anthropogenic emissions released in the MMA [20]. This is a result of a relatively high proportion of vehicles per inhabitant registered in this urban center (approximately one vehicle for every two inhabitants).

2. Methods: Database and analysis tools

The study used data collected by the *Sistema Integral de Monitoreo Ambiental* (SIMA; Integrated Environmental Monitoring System) of the MMA. At the time of the study, valid data from six operational routine air quality stations were available: Downtown, Southeast, Southwest, Northeast, Northwest, and North (see Figure 1). Data archived for the period of August 2012 to August 2013 were retrieved. The database contained hourly-average concentrations of CO, NO, NO_2, and O_3, as well as meteorological parameters (relative humidity, atmospheric pressure, dry bulb temperature, solar radiation [SR], wind speed [WS], and wind direction [WD]). These data go through a quality assurance/quality control process defined by SIMA in compliance with international standards. Additional air quality parameters monitored by the stations (mainly, SO_2 and particulate matter with aerodynamic diameter less than or equal to 10 microns [PM_{10}] and less than or equal to 2.5 microns [$PM_{2.5}$]) were not used in this study, as the focus was on the relationship between O_3 and NO_x.

In addition to the above chemical parameters, NO_y was monitored in the Downtown station from August 2012 to August 2013, using a NO-NO_y (Thermo Scientific, Model 42i-Y) chemiluminescence continuous sampling device. NO_y is a chemical parameter that is not routinely measured by Mexican air quality stations, as it is not considered a criteria pollutant. The decision to deploy the NO-NO_y instrument at the location of the Downtown station was based on spatial homogeneity studies performed in the past for the MMA [22], which indicate that pollutant levels observed in the Downtown station are representative of the MMA, with the exception of the Southeast region. The data collected by the NO-NO_y device went through a validation process similar to that routinely conducted by SIMA on its own collected data. The main conditions to reject data included the following red flags: obstructed capillary tubing, low flow in the inlet, and concentrations outside the measurement range (i.e., above 200 ppbv). The data were then consolidated and analyzed on a daily basis, a monthly basis, and by seasons (Summer

http://dx.doi.org/10.5772/59752

and Fall 2012, and Winter, Spring, and Summer 2013). Summer 2012 included only data from August and September of 2012; Summer 2013 did not include data for September 2013.

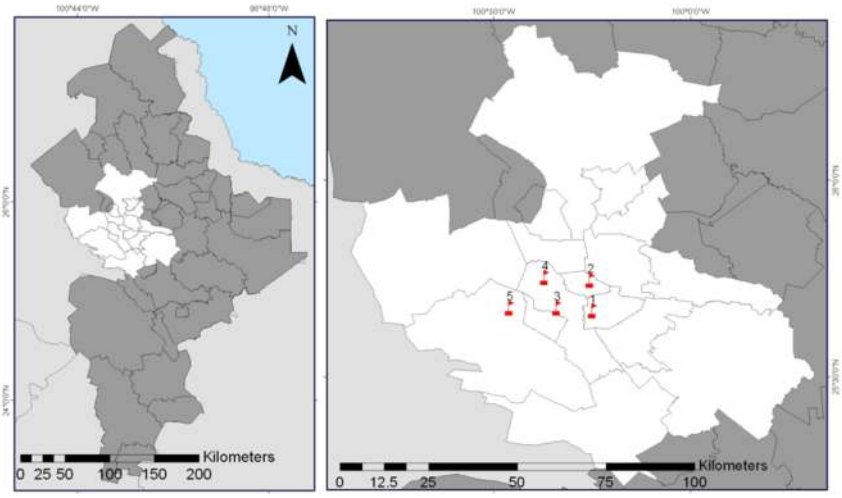

Figure 1. Municipalities that comprise the Monterrey Metropolitan Area (left panel) and location of the air quality stations monitoring stations used in this study (right panel): 1 Southeast, 2 Northeast, 3 Downtown, 4 Northwest, 5 Southwest; data from the North station was not used

Once the data were consolidated, an exploratory analysis of the data set was conducted to derive descriptive statistics. In addition, correlation analysis was conducted to explore relations between the chemical and meteorological parameters, with emphasis on the relationships among O_3, NO_x, and NO_y. This analysis was complemented by the use of polar plots and wind roses to determine the relationship between high pollutant levels and transport conditions (wind speed and direction).

Grouping techniques were then applied for further exploration of the data. Two methods were used: Principal Components Analysis (PCA) and Analysis of Variance (ANOVA). PCA is helpful in reducing the dimensionality of the dataset, and ANOVA can identify differences among data groups. Thus, PCA was used to identify the most important variables in the dataset which in turn merit further exploration. With the ANOVA, we attempted to determine differences in the weekday and weekend conditions that resulted in high O_3 levels. All statistical analyses were conducted using Minitab® 16, and plots were constructed using the R programming language.

3. Results

3.1. Descriptive statistics

Table 1 summarizes the descriptive statistics of the chemical and meteorological parameters retrieved from the Downtown air quality monitoring station. The values presented are based

on the daily means for the August 2012-August 2013 period. The climatology of the MMA is portrayed in these results: a hot semi-arid region characterized by extreme weather conditions [23]. The long-term average temperature of Monterrey is around 23°C, with temperatures that can reach 40°C in summer and below 0°C in winter. Average humidity is 62%; the rainy season is between August and October, directly related to the occurrences of hurricanes in the Gulf of Mexico (the average mean annual precipitation is around 600 mm). Due to its geographic location, the MMA is influenced by anti-cyclonic systems from the Gulf of Mexico [24], which in some instances result in high atmospheric stability in the region, thereby inhibiting the vertical mixing of pollutants.

Species/Parameters	Mean ± Std. Dev.	Median	Maximum	Minimum
O_3 (ppb)	25.7 ± 9.0	24.4	50.7	2.6
NO_2 (ppb)	16.3 ± 5.9	15.3	39.2	3.3
NO (ppb)	6.5 ± 4.7	5.3	34.4	0.6
NO_y (ppb)	40.0 ± 20.3	35.2	188.2	12.1
CO (ppm)	0.78 ± 0.26	0.75	1.78	0.21
Solar radiation (kW/m^2)	0.24 ± 0.12	0.24	0.70	0.00
Temperature (°C)	24.4 ± 5.2	25.8	32.5	9.5
Wind speed (km/h)	1.84 ± 0.47	1.84	3.21	0.71
Relative Humidity (%)	62.9 ± 16.8	64.17	98.9	13.5

Table 1. Descriptive statistics for parameters monitored at the Downtown air quality station of the MMA (annual means, medians, maximum values, and minimum values of the daily averages)

Details of the monthly variation of the daily averages of the chemical and meteorological parameters are depicted in Figure 2. O_3 levels tend to be the highest during springtime, as well as during late summer and early fall. These periods correspond to the times when temperature and SR are high and wet precipitation is low, i.e., conditions that foster photochemical reactions. Another relevant feature presented in Figure 2 involves the inverse relationship observed between O_3 and NO_x. That is, during the cold months, when SR is low, NO_x levels tend to be high due to inhibition of the reactions between VOCs and NO_x that promote the conversion of NO to NO_2, as well as suppression of the photo-dissociation of NO_2 to produce O_3. We need to bear in mind that NO_x emissions are mainly in the form of NO. Thus, an accumulation of NO and NO_2 is observed in winter. At other times, temperatures and SR increase, promoting photochemical reactions. A meteorological component influences the observed NO_x concentrations: shallow mixing heights and low wind speeds during winter. The O_3 seasonal boxplots indicate that even though fall is the second most important season with respect to the frequency of peak O_3 levels, it is also the time when the average O_3 is the lowest (Figure 3). This can be explained by the incidence of rain events associated with this season.

http://dx.doi.org/10.5772/59752

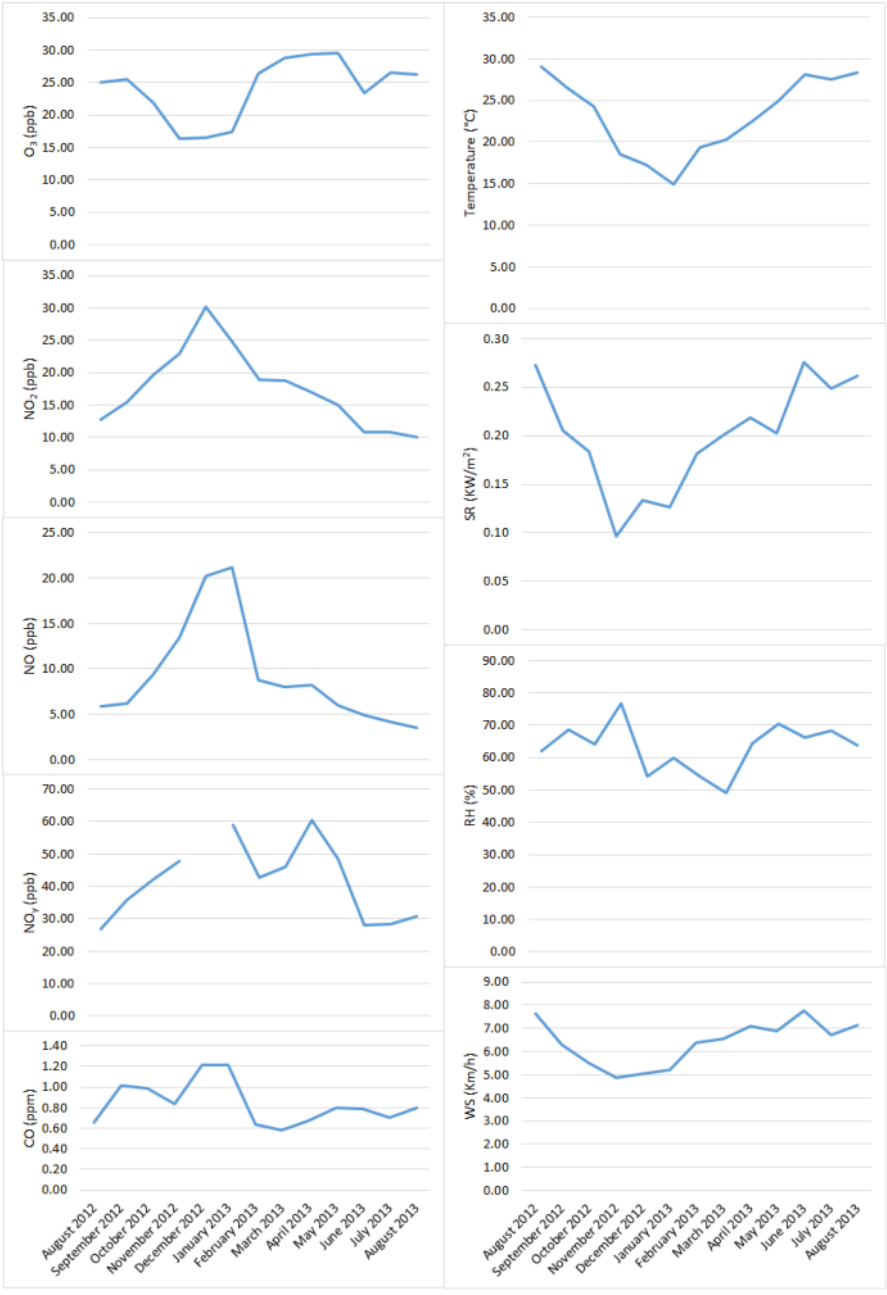

Figure 2. Time series plots of monthly averages of the mean daily values of chemical and meteorological parameters observed at the Downtown station

3.2. Spatial analysis

The exploratory analysis was complemented by the construction of bivariate polar plots of NO_x (see Figure 4) and wind roses (see Figure 5) for five of the six air quality monitoring stations, covering the main sub-regions of the MMA. The five selected stations correspond to typical upwind locations (Northeast and Southeast), Downtown Monterrey, and typical downwind locations (Northwest and Southwest), as illustrated in Figure 5. Seasonal variation is also presented in these plots.

The polar plots represent NO_x concentration as a function of wind speed and direction, and they help identify the possible occurrence/prevalence of horizontal transport conditions that lead to high NO_x events. Further away from the center of the plot, the wind speed is higher. The form of the polar plot can provide an indication of the wind direction and speed frequency; however, this information is better observed through the corresponding wind roses.

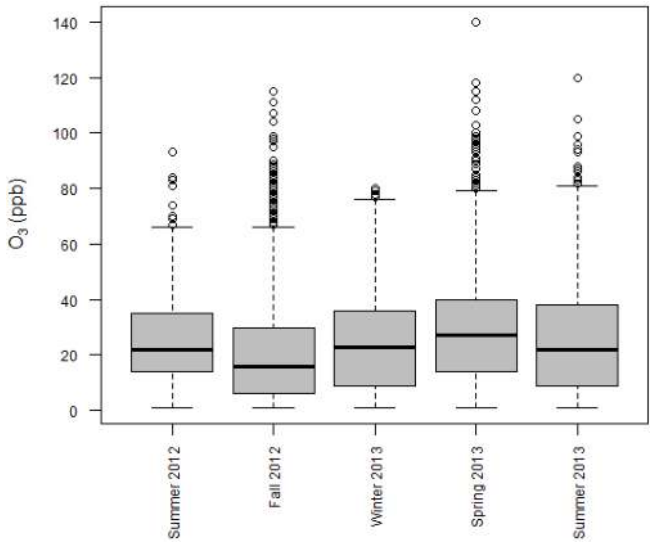

Figure 3. O_3 boxplots by seasonal periods for 1-hr average values reported at the Downtown station

In general, Figure 4 indicates higher transport of NO_x from the northern stations (this can be catalogued as "fresh" NO_x), which then is consumed as the air masses traverse the urban core. The transport patterns appear to be similar in all seasons. Thus, the change in NO_x by season appears to be more strongly linked to photochemical conditions (temperature and SR) than to wind patterns.

Using the same analysis as was used for NO_x, Figure 6 depicts the behavior of O_3 as a function of wind speed and direction exclusively at the Downtown station. In all cases, the higher concentrations begin to occur when the wind velocity was above 2 m/s, indicating the influence of transport and aging of air masses on the observed O_3 concentrations and weak O_3 production

http://dx.doi.org/10.5772/59752

under stagnant conditions. Transport influences the levels of O_3; consequently, the highest O_3 levels correlate with the prevailing wind directions (wind blowing from the Northeast-East-Southeast and from the North-Northwest-West). The East-to-West air flow channels air masses through the long axis of the MMA, adding more precursors to the chemically aged mixtures as they traverse the urban core, thereby promoting O_3 production.

The frequency of high O_3 concentrations related to a specific wind direction cannot be inferred from the polar plots, however. That analysis was conducted by constructing boxplots for 1-hr average O_3 concentrations for the three main wind categories (classified based on direction from which the wind was blowing) and segregated by season (see Figure 7). The year around the peak O_3 concentrations and the maximum 1-hr average concentrations occur when the wind blows from the Northeast-East-Southeast. O_3 levels, on average, are lower when the wind blows from the North-Northwest-West, and they are the lowest when winds blow from the South-Southeast (with the exception of the summer, when this direction provides higher average concentrations than the North-Northwest-West direction).

Comparison of the O_3 levels presented by the polar plots (Figure 6) for spring and fall indicates that the influence of transport is less important during fall than in spring, as wind speeds tend to be lower; high O_3 events are mainly related to events when the speed is in the range of 2.0-3.5 m/s. In spring, O_3 levels can remain high at wind speeds above 4 m/s.

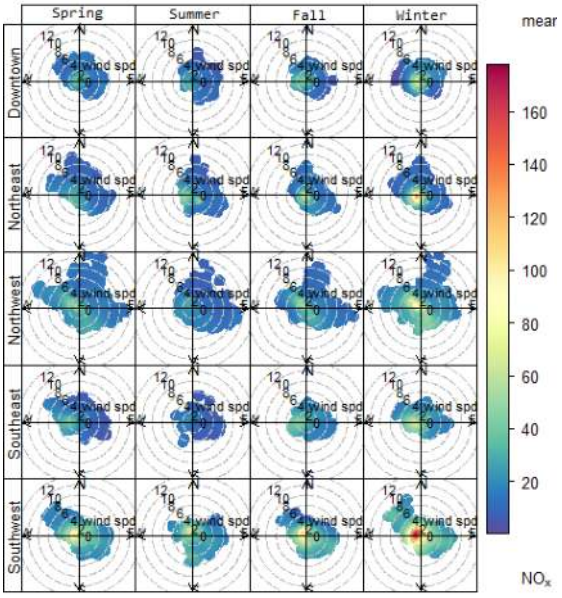

Figure 4. Polar plot for 1-h average NO_x concentrations at five different monitoring stations within the MMA (the radial dimension is an indication of increasing wind speed [m/s])

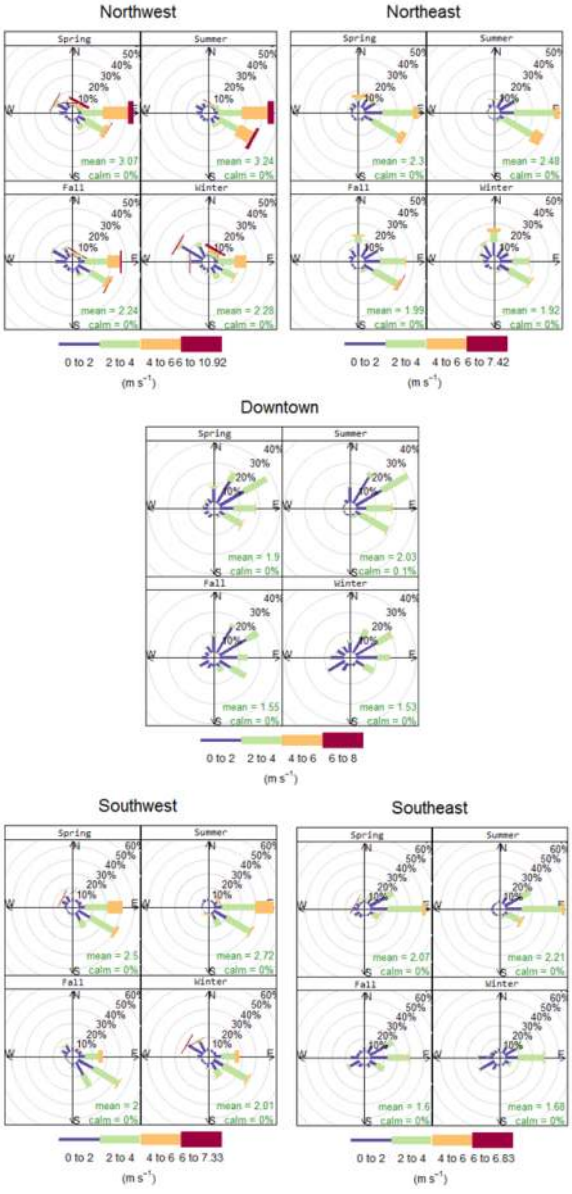

Figure 5. Wind roses at five different monitoring stations within the MMA

http://dx.doi.org/10.5772/59752

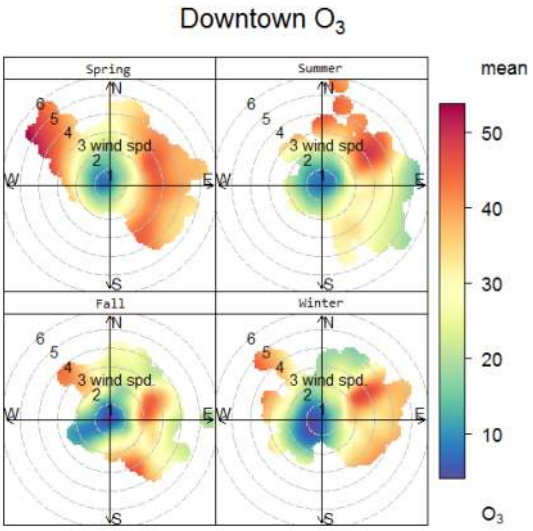

Figure 6. Polar plot for 1-h average O_3 concentrations at five different monitoring stations within the MMA (the radial dimension is an indication of increasing wind speed [m/s])

3.3. Regression analysis

Figure 2 gives an initial indication of a direct relationship between NO and NO_2 levels and an inverse relationship between NO_x and O_3 levels. This was explored further by means of scatter plots (not presented for brevity), which were used to derive linear regression expressions among NO_x constituents and between NO_x and O_3:

$$\left[NO_x\right] = 1.5\left[NO\right] + 13.0 \tag{11}$$

$$\left[O_3\right] = -0.37\left[NO_x\right] + 34 \tag{12}$$

where [*i*] represents the molar concentration of species i. Here, the 1-hr average concentrations were used to derive equations (11) and (12). These expressions corroborate prior findings. The relevance of equation (12) is that it provides a measure of the expected, first order change in O_3 provided by a change in NO_x concentration (which can occur from a change in NO emissions). The results indicate that O_3 would, in fact, increase as NO_x tends to be reduced. This counterintuitive finding is a well-known result seen in urban areas dominated by a VOC-sensitive regime [25]. Other studies that have used complex photochemical air quality models have reached similar conclusions. Downtown Monterrey appears to be dominated by a VOC-sensitive regime in which VOC controls would work better for reducing O_3 levels [20].

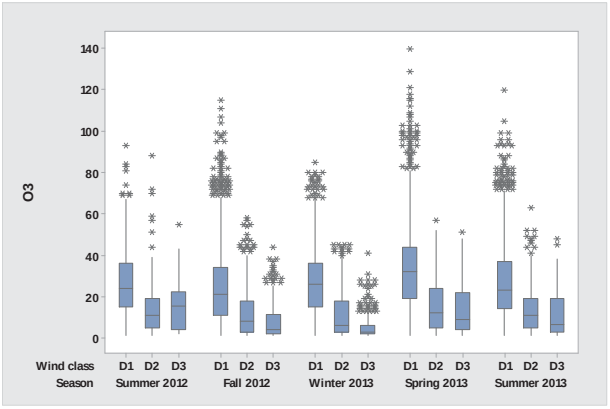

Figure 7. Boxplots of 1-hr averaged O_3 concentrations observed at the Downtown station, classified by prevailing wind direction: D1 (wind blowing from 20 to 120°), D2 (wind blowing from 270 to 360°), and D3 (wind blowing from 180 to 150°)

3.4. Analysis of NO_y levels

Up to this point, our analysis has focused on describing the relationship between NO_x and O_3 production based on the meteorological conditions that foster photochemical reactions. The generalized chemical mechanism that describes this relationship indicates that other reaction products can be of interest in describing the dynamics of O_3 production. In particular, the levels of NO_y provide additional information and serve as an indicator of the degree to which the air masses have been subjected to photochemical processing (aging), thereby providing information on O_3 production.

Table 2 presents the results of the correlation analysis of different chemical and meteorological parameters with NO_y. A correlation coefficient (R^2) of NO_2 with NO_y above 0.78 is noted for months in which O_3 production is not the highest, and between 0.40 and 0.68 for the months with the highest O_3 production. In general, a high percentage of NO_y corresponds to NO_x (Figure 2); thus, the response of one clearly depends on the other.

The difference between NO_y and NO_x (known as NO_z) includes the inorganic and organic nitrates derived from photochemical processing of the NO_x-VOCs mixtures. The typical composition of NO_z is approximately 50%-55% HNO_3, 35%-40% PAN, 1%-5% HNO_2, and a marginal contribution of other nitrates [26, 27]. During the cold months, the production of NO_z can be inhibited by meteorological conditions that do not foster photochemical reactions. Thus, the relative contribution of NO_x to NO_y is the highest, and, therefore, the responses of both species are expected to show high correlation. When conditions favor O_3 production, more NO_z is produced, thereby limiting the contribution of NO_x to the total NO_y. Consequently, the level of correlation drops as the nonlinear photochemistry and sinks of NO_y increase in importance. Of interest is the fact that during spring, the season with the highest peak O_3 1-hr concentrations, the correlation of NO_x species with NO_y is the lowest. A similar response is obtained between CO and NO_y, which can be explained by the typical strong correlation

http://dx.doi.org/10.5772/59752

between CO and NO_x emissions, particularly in urban areas that are heavily influenced by mobile-source emissions. With respect to meteorological variables, the highest correlation was with wind speed, and, as in the case of NO_x and CO, the correlation was the lowest during spring.

	Summer 2012	Fall 2012	Winter 2013	Spring 2013	Summer 2013
NO_2 (ppbv)	0.811 (< 0.001)	0.676 (< 0.001)	0.819 (< 0.001)	0.411 (< 0.001)	0.783 (< 0.001)
NO (ppbv)	0.335 (< 0.001)	0.610 (< 0.001)	0.661 (< 0.001)	0.275 (< 0.001)	0.615 (< 0.001)
O_3 (ppbv)	0.031 (< 0.001)	0.106 (< 0.001)	0.151 (< 0.001)	0.065 (< 0.001)	0.070 (< 0.001)
CO (ppmv)	0.764 (< 0.001)	0.420 (< 0.001)	0.664 (< 0.001)	0.227 (< 0.001)	0.712 (< 0.001)
Solar radiation (kW/m^2)	0.011 (< 0.001)	0.001 (0.639)	0.004 (0.052)	0.001 (0.165)	0.009 (< 0.001)
Temperature (°C)	0.009 (0.048)	0.024 (< 0.001)	0.022 (< 0.001)	0.005 (0.002)	0.063 (< 0.001)
Wind speed (km/h)	0.252 (< 0.001)	0.247 (< 0.001)	0.203 (< 0.001)	0.112 (< 0.001)	0.225 (< 0.001)

Table 2. Correlation coefficients (R^2) of parameters monitored by the SIMA downtown station with NO_y (in parenthesis *p*-values at an α of 0.05)

The results of the correlation analysis suggest a relationship between NO_x and NO_y, but a correlation between NO_y and O_3 is less evident. Figure 2 shows two peaks in the annual cycle of the NO_y monthly average concentration (constructed from daily NO_y average concentrations). One peak occurs during the cold months and is associated with the high levels of NO_x (low NO_z component), while the second peak appears during spring, which is the period with highest photochemical activity (highest O_3 levels); thus, as NO_x is consumed, and its levels decrease and NO_y levels are high, NO_z must be contributing heavily to NO_y. The peaks of NO_y are associated with different conditions, so we looked in greater detail into the seasonal levels of NO_y. Figure 8 depicts the 1-hr NO_y concentrations by season. The highest levels (both of peak and season-average concentrations) occur in winter, followed by fall and spring (when O_3 is the highest), with summer registering the lowest levels. The O_3 levels presented in Figure 3 do not appear to track the NO_y levels.

We then attempted to determine a clearer relationship between O_3 and NO_y by conducting a Principal Components Analysis (PCA) (see Table 3). The first principal component (PC1) has to do with O_3 precursors in the form of primary emissions or intermediate products (NO_x, NO_y, and CO), in line with the results from the descriptive statistics. The second principal component (PC2) covers photochemical O_3 production (O_3 and solar radiation). The third principal component (PC3) refers to a combined meteorological effect that includes horizontal

transport (wind direction) and temperature— an effect that was also observed in the descriptive statistics results. The first two principal components represent almost 60% of the variance.

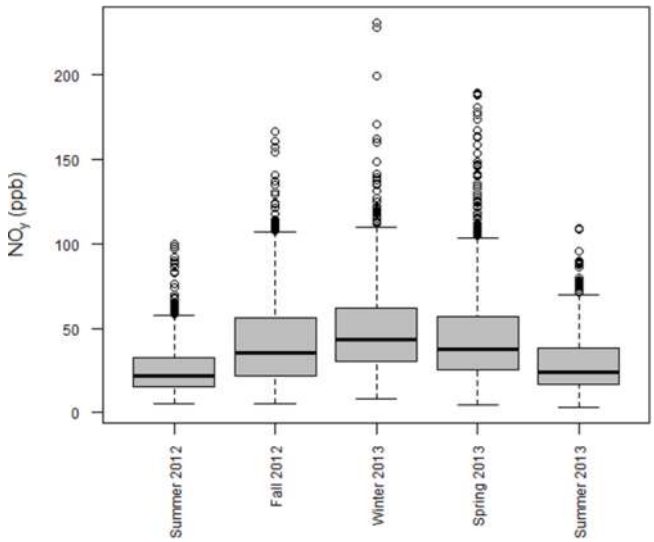

Figure 8. Annual average distribution of NO_y concentrations

Component	PC1	PC2	PC3
NO_y	**0.481**	0.055	–0.009
NO_2	**0.387**	0.087	–0.123
NO	**0.375**	0.029	0.151
O_3	–0.226	**0.447**	0.075
CO	**0.400**	0.110	0.081
Solar radiation	–0.090	**0.497**	0.031
Temperature	–0.197	0.370	**0.411**
Wind velocity	–0.288	0.276	0.084
Wind speed	0.175	0.339	**0.794**
Accumulated variance (%)	0.395	0.595	0.672

Table 3. Principal components analysis results

Given these results, we conducted an additional assessment on the effects of meteorological parameters on O_3 and NO_y levels, which showed the effects of horizontal transport. O_3, temperature, wind speed, and wind direction data were particularly correlated (see Table 4). In addition, complementary polar plots were constructed for NO_y (Figure 9). The highest correlation between O_3 and wind speed occurred during the winter of 2013. In this case, the

http://dx.doi.org/10.5772/59752

slope of the linear regression was positive (i.e., as the wind speed increases, O_3 also increases). In a similar way, the highest correlation between O_3 and wind direction occurred during the winter of 2013. This indicates that transport is a major factor responsible for the average O_3 levels observed in the winter in the MMA. The polar plot for NO_y confirms that high levels of NO_y during winter (which are, as discussed, mostly NO_x) are associated with low wind speeds. This relationship between NOy and wind speed would indicate that NO_x is not being processed and translated to high local production of O_3 in the winter.

			Wind speed		
	Summer 2012	Fall 2012	Winter 2013	Spring 2013	Summer 2013
R^2	0.212	0.271	0.350	0.025	0.231
Slope	2.348	3.625	3.342	1.164	2.986
Intercept	6.836	0.937	3.319	35.560	4.850
p-value	< 0.001	< 0.001	< 0.001	< 0.001	< 0.001
			Winddirection		
	Summer 2012	Fall 2012	Winter 2013	Spring 2013	Summer 2013
R^2	0.001	0.022	0.216	0.002	0.010
Slope	–0.005	–0.031	–0.088	0.014	–0.027
Intercept	25.432	24.893	35.313	44.662	28.428
p-value	< 0.001	< 0.001	< 0.001	< 0.001	< 0.001
			Temperature		
	Summer 2012	Fall 2012	Winter 2013	Spring 2013	Summer 2013
R^2	0.454	0.327	0.341	0.344	0.536
Slope	2.834	1.877	2.017	2.031	3.792
Intercept	–57.407	–21.939	–14.324	–5.969	–81.202
p-value	< 0.001	< 0.001	< 0.001	< 0.001	< 0.001

Table 4. O_3 correlations with meteorological parameters (*p*-values at an α of 0.05)

An additional way to establish the influence of transport on the levels of air pollutants is to analyze the CO-to-NO_y ratio. Values close to 10 are indicative of an influence of local sources, and ratios larger than 100 indicate the influence of regional (remote) sources [11]. Figure 10 depicts the CO-to-NO_y ratios observed at the Downtown station as a function of the season. The average ratio tends to be the inverse with respect to the behavior of the average levels of NO_y, although one main difference exists: the lowest ratios are observed during winter but also during spring, intermediate values are observed during the fall, and the highest average values are registered during the summer. In a few cases, the CO-to-NO_y ratio reached values of 100 or more, and the 95th percentile, in general, was below 56. Thus, air pollution in the MMA during winter appears to be heavily influenced by low wind conditions (Figure 2 indicates the lowest average wind speeds during this season), and poor photochemical activity limits the levels of NO_z and O_3. The O_3 levels that are registered are characteristic of background amounts

that are transported to the urban center when wind speeds are sufficiently strong. The spring level is also heavily influenced by local emissions, but meteorological conditions do favor photochemical activity, resulting in production of the highest levels of O_3. Fall would seem to be influenced partly by local emissions and partly by transport. Finally, summer is characterized by the influence of more regional (and aged) emissions. During the first two months of the summer season, the ambient conditions tend to be characterized by high temperatures and deep planetary boundary layers that promote vertical mixing. In addition, conditions favor the mixing of these vertical columns with pollutants that undergo long-range transport.

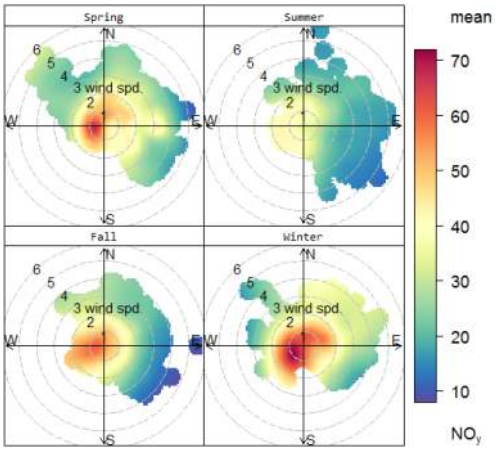

Figure 9. Polar plot for NO_y at the Downtown monitoring station

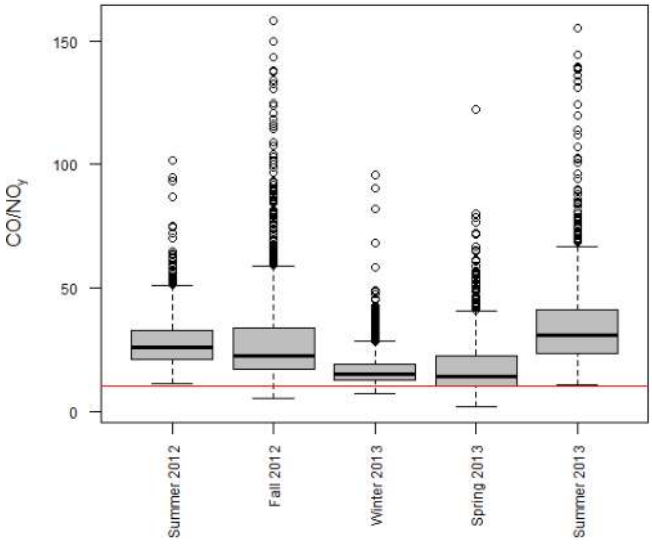

Figure 10. Seasonal variation of CO-to-NO_y ratios (the red line represents a value of 10 for the ratio)

http://dx.doi.org/10.5772/59752

3.5. Weekend-weekday effect

A final aspect of interest in this study was to define if a weekend-weekday effect could be established based on NO_x and NO_y readings. Previous studies have demonstrated that O_3 levels in urban centers can be higher during weekends [28, 29], a condition that might be thought of as counterintuitive, as emissions from anthropogenic sources tend to be lower during weekends. An explanation for the occurrence of this weekend-weekday effect can be obtained by analyzing the photochemical mechanism for the production of O_3. Urban centers tend to be VOC-sensitive; that is, NO_x is in excess and, thus, processes that remove NO_2 from the reactive mixtures are promoted. For example, NO_2 efficiently scavenges $HO^{\bullet}$ radicals through reaction 9, producing HNO_3, which is a direct sink for NO_x. This limits the reaction of $HO^{\bullet}$ radicals with VOCs, which, in turn, controls the production pathways for O_3. During weekends, the ratio at which VOCs and NO_x are emitted can change, preferentially reducing the emissions of NO_x. If this happens, less NO_x is available in the atmosphere, reaction 9 becomes less important, more $HO^{\bullet}$ radicals become available to react with the VOCs, and, thus, O_3 tends to increase. Figure 11 illustrates the distribution of NO_y concentrations by day of the week. At a first glance, NO_y values tend to be quite constant throughout the day. However, Tuesdays and Wednesdays present the lowest peak values, while average levels on Sunday tend to be lower than during the rest of the week. If the average NO_x-to-NO_y ratio is examined, values tend to be lower during the weekends (Figure 12). The NO_x-to-NO_y ratio provides information on the level of photochemical processing of the observed air parcels. Ratios closer to 1 would indicate that most of the NO_y is in the form of NO_x, and thus, it could imply the presence of fresh emissions or the transport of unprocessed emissions. As the ratio drops, the relative contribution of NO_z increases, indicating that an aged (photochemically processed) air parcel is being observed.

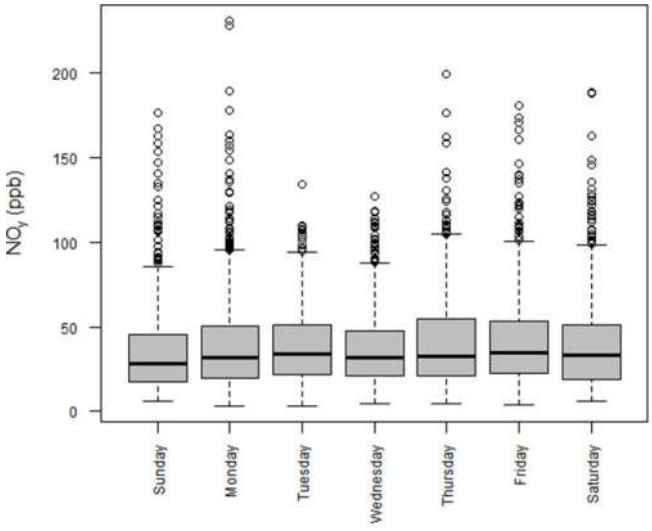

Figure 11. Boxplot for NO_y levels by day of the week

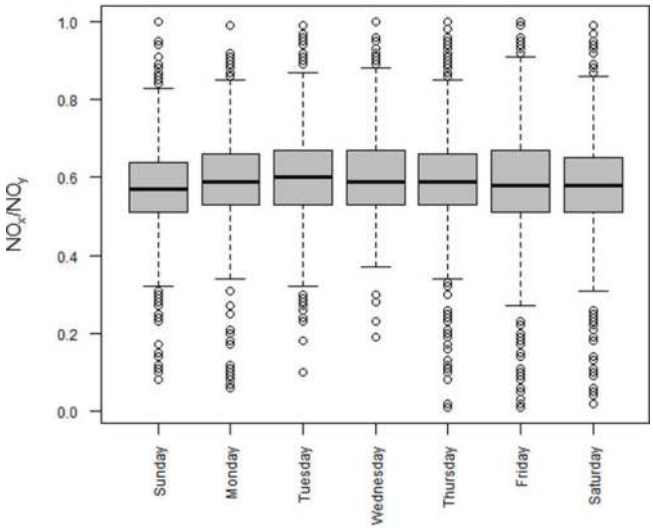

Figure 12. Boxplot for the NO_x-to-NO_y ratio by day of the week

Finally, we conducted an Analysis of Variance (ANOVA) test for the NO_x-to-NO_y ratio by season (see Table 5). For the hot months (spring and summer), lower ratios were observed during weekends compared to weekdays. In fact, the lowest average ratio was obtained during spring, the season with the highest average and peak O_3 concentrations. In contrast, the winter of 2013 showed a marginally higher ratio during the weekends than on the weekdays, but the difference was not statistically significant. This could be the result of an intensive use of fuels during the whole week in response to the low temperatures. For the fall of 2012, this statistical test also indicates no difference between weekdays and weekends. Fall, as the results from previous sections suggest, is influenced by days with high O_3 production and days with very low O_3 levels as a result of the transition from a period with high SR and temperature to the regional rainy season.

Season	Average ± Standard Dev. (Weekdays)	Average ± Standard Dev. (Weekends)	*p-value*	Difference between Weekdays and Weekends
Summer 2012	0.606 ± 0.139	0.582 ± 0.124	0.033	Yes
Fall 2012	0.671 ± 0.141	0.668 ± 0.107	0.657	No
Winter 2013	0.545 ± 0.086	0.549 ± 0.077	0.504	No
Spring 2013	0.553 ± 0.112	0.496 ± 0.142	< 0.001	Yes
Summer 2013	0.586 ± 0.110	0.561 ± 0.112	< 0.001	Yes

Table 5. Results of the ANOVA test for the NO_x-to-NO_y ratio (*p*-values are at an α of 0.05)

http://dx.doi.org/10.5772/59752

4. Conclusions

Observational-based methods have proven valuable for analysis of the chemical interactions that give rise to high air pollution events in urban areas. In particular, the vast amount of information gathered by networks of air quality stations can provide insight into the production of secondary air pollutants such as O_3, as atmospheric conditions change throughout the year. This analysis can be enhanced if complementary observations are also made of species that are not routinely registered, such as NO_y.

In this study, we presented a statistical analysis performed on the air quality and meteorological data registered by the routine air quality stations of the MMA. The analysis included descriptive statistics, regression analysis, correlation analysis, PCA, and ANOVA, along with the interpretation of bivariate polar plots, wind roses, and boxplots. In addition, ratios of NO_x with NO_y and CO with NO_y provided additional information on the level of chemical processing of the air masses traversing the MMA. When used together, these techniques prove to be complementary, thus providing more robust results.

In the MMA, O_3 registers two distinct annual peaks: one in spring and the other in late summer-early fall. The analysis of meteorological conditions and air pollutant levels indicate that the O_3 concentrations during winter would be characteristic of background conditions that get transported to the urban center when wind speeds are sufficiently strong. O_3 production in winter is small because typical conditions that foster photochemical activity are not present, such as relatively high temperatures and strong solar radiation. During this season, NO_y is composed mainly of locally-emitted NO_x, which corroborates the low photochemical activity. That is, the ambient conditions do not favor the catalytic effect of NO_x to produce O_3. Spring is also heavily influenced by local emissions, but meteorological conditions favor photochemical activity, leading to production of the highest levels of O_3. In this season, winds bring background O_3 to the MMA, and precursors traverse the long-axis of the urban core, allowing for chemical processing, injection of fresh emissions, and high photochemical production. Spring registers the highest amount of NO_z, indicating that NO_x is reacting efficiently with VOCs to produce photochemical oxidants, including O_3. Fall would seem to be influenced partly by local emissions and partly by transport. Even though fall has the second highest peak O_3 levels, the average O_3 in this season is relatively low. This can be explained by the fact that the rainy season occurs during this period. Finally, summer would be characterized by the influence of more regional (and aged) emissions. Deep planetary boundary layers are characteristic of this season, allowing mixing and dispersion of air pollutants that result in the lowest NO_y levels of the year. Thus, even though temperature and solar radiation levels could suggest high O_3 production, photochemical activity is limited by transport and mixing effects. Finally, for the hot months (spring and summer), a distinct weekday-weekend effect can be identified, as the NO_x-to-NO_y ratio tends to be higher during weekdays than during weekends. This would indicate changes in NO_x emission rates during the week, which could lead to higher O_3 events during the weekend, in line with the VOC-sensitive condition of the MMA atmosphere that has been suggested by others.

Overall, the analysis of NO_x and NO_y levels with other chemical and meteorological variables as well as the correlation and ratios between NO_x and NO_y provide indicators of the level of photochemical activity that fosters O_3 production.

Acknowledgements

This study was supported by the Mexican Council for Science and Technology (CONACYT) through grant No. CB-2010-1-154122. Additional support was received from Tecnológico de Monterrey through grant no. CAT-186. E. Carrillo appreciates the scholarship received from CONACYT during his research stay (MSc) at Tecnológico de Monterrey.

Author details

Alberto Mendoza* and Edson R. Carrillo

*Address all correspondence to: mendoza.alberto@itesm.mx

School of Engineering and Sciences, Tecnológico de Monterrey, Monterrey, Mexico

References

[1] Seinfeld JH. Urban Air Pollution: State of the Science. Science 1989; 243(4892) 745-752.

[2] Atkinson R. Atmospheric chemistry of VOCs and NOx. Atmospheric Environment 2000; 34(12–14) 2063-2101.

[3] Yang C, Yang H, Guo S, Wang Z, Xu X, Duan X, Kan H. Alternative ozone metrics and daily mortality in Suzhou: The China Air Pollution and Health Effects Study (CAPES). Science of The Total Environment 2012; 426: 83-89.

[4] Ha S, Hu H, Roussos-Ross D, Haidong K, Roth J, Xu X. The effects of air pollution on adverse birth outcomes. Environmental Research 2014; 134: 198-204.

[5] Vlachokostas C, Nastis SA, Achillas C, Kalogeropoulos K, Karmiris I, Moussiopoulos N, Chourdakis E, Banias G, Limperi N. Economic damages of ozone air pollution to crops using combined air quality and GIS modelling. Atmospheric Environment 2010; 44(28) 3352-3361.

[6] Feng Z, Sun J, Wan W, Hu E, Calatayud V. Evidence of widespread ozone-induced visible injury on plants in Beijing, China. Environmental Pollution 2014; 193: 296-301.

[7] Fang Y, Naik V, Horowitz LW, Mauzerall DL. Air pollution and associated human mortality: the role of air pollutant emissions, climate change and methane concentration increases from the preindustrial period to present. Atmospheric Chemistry and Physics 2013; 13(3) 1377-1394.

[8] Seinfeld JH, Pandis SN. Atmospheric Chemistry and Physics: From Air Pollution to Climate Change. 2nd ed. Hoboken, New Jersey: John Wiley & Sons.; 2006.

[9] Warnek P. Chemistry of the Natural Atmosphere. International Geophysics Series. New York: Academic Press. 757; 1988.

[10] Russell A, Dennis R. NARSTO critical review of photochemical models and modeling. Atmospheric Environment 2000; 34(12–14) 2283-2324.

[11] Kleanthous S, Vrekoussis M, Mihalopoulos N, Kalabokas P, Lelieveld J. On the temporal and spatial variation of ozone in Cyprus. Science of The Total Environment 2014; 476–477: 677-687.

[12] Nishanth T, Praseed KM, Kumar MKS, Valsaraj KT. Influence of ozone precursors and PM_{10} on the variation of surface O_3 over Kannur, India. Atmospheric Research 2014; 138: 112-124.

[13] Iqbal MA, Kim K-H, Shon Z-H, Sohn J-R, Jeon E-C, Kim Y-S, Oh J-M. Comparison of ozone pollution levels at various sites in Seoul, a megacity in Northeast Asia. Atmospheric Research 2014; 138: 330-345.

[14] Zhang Y, Mao H, Ding A, Zhou D, Fu C. Impact of synoptic weather patterns on spatio-temporal variation in surface O_3 levels in Hong Kong during 1999–2011. Atmospheric Environment 2013; 73: 41-50.

[15] Alghamdi MA, Khoder M, Harrison RM, Hyvärinen AP, Hussein T, Al-Jeelani H, Abdelmaksoud AS, Goknil MH, Shabbaj II, Almehmadi FM, Lihavainen H, Kulmala M, Hämeri K. Temporal variations of O_3 and NO_x in the urban background atmosphere of the coastal city Jeddah, Saudi Arabia. Atmospheric Environment 2014; 94: 205-214.

[16] Jenkin ME. Investigation of the impact of short-timescale NO_x variability on annual mean oxidant partitioning at UK sites. Atmospheric Environment 2014; 90: 43-50.

[17] Hassan IA, Basahi JM, Ismail IM, Habeebullah TM. Spatial Distribution and Temporal Variation in Ambient Ozone and Its Associated NO_x in the Atmosphere of Jeddah City, Saudi Arabia. Aerosol and Air Quality Research 2013; 13 1712-1722.

[18] González-Santiago O, Badillo-Castañeda CT, Kahl JDW, Ramírez-Lara E, Balderas-Renteria I. Temporal Analysis of PM_{10} in Metropolitan Monterrey, México. Journal of the Air & Waste Management Association 2011; 61(5) 573-579.

[19] Sistema Integral de Monitoreo Ambiental. Estadística SIMA: Gobierno del Estado de Nuevo León. http://www.nl.gob.mx/?P=med_amb_mej_amb_sima_estadisti (accessed 1 Oct 2013).

[20] Sierra A, Vanoye AY, Mendoza A. Ozone sensitivity to its precursor emissions in northeastern Mexico for a summer air pollution episode. Journal of the Air & Waste Management Association 2013; 63(10) 1221-1233.

[21] Green J, Sánchez S. Air Quality In Latin America: An Overview. Washington, DC: Clean Air Institute; 2013. http://www.cleanairinstitute.org/calidaddelaireamericalatina/ cai-report-english.pdf (accessed 22 September 2014).

[22] Mancilla Y. $PM_{2.5}$ Source Apportionment using Partial Least Squares Based on Organic Molecular Markers: Monterrey Metropolitan Area, Mexico. PhD thesis. Tecnológico de Monterrey; 2013.

[23] SEMARNAT, Gobierno del Estado de Nuevo León. Programa de Gestión para Mejorar la Calidad del Aire del Área Metropolitana de Monterrey 2008-2012. 2008. http://www.semarnat.gob.mx/archivosanteriores/temas/gestionambiental/calidaddelaire/Documents/Calidad%20del%20aire/Proaires/ProAires_Vigentes/6_ProAire%20AMM%202008-2012.pdf (accessed 23 September 2014).

[24] Rodwell MJ, Hoskins BJ. Subtropical Anticyclones and Summer Monsoons. Journal of Climate 2001; 14(15) 3192-3211.

[25] Sillman S. The relation between ozone, NO_x and hydrocarbons in urban and polluted rural environments. Atmospheric Environment 1999; 33(12) 1821-1845.

[26] Luke WT, Kelley P, Lefer BL, Flynn J, Rappenglück B, Leuchner M, Dibb JE, Ziemba LD, Anderson CH, Buhr M. Measurements of primary trace gases and NO_y composition in Houston, Texas. Atmospheric Environment 2010; 44(33) 4068-4080.

[27] Luecken DJ, Tonnesen GS, Sickles IJE. Differences in NO_y speciation predicted by three photochemical mechanisms. Atmospheric Environment 1999; 33(7) 1073-1084.

[28] Wang YH, Hu B, Ji DS, Liu ZR, Tang GQ, Xin JY, Zhang HX, Song T, Wang LL, Gao WK, Wang XK, Wang YS. Ozone weekend effects in the Beijing–Tianjin–Hebei metropolitan area, China. Atmospheric Chemistry and Physics 2014; 14 2419-2429.

[29] Warneke C, de Gouw JA, Edwards PM, Holloway JS, Gilman JB, Kuster WC, Graus M, Atlas E, Blake D, Gentner DR, Goldstein AH, Harley RA, Alvarez S, Rappenglueck B, Trainer M, Parrish DD. Photochemical aging of volatile organic compounds in the Los Angeles basin: Weekday-weekend effect. Journal of Geophysical Research: Atmospheres 2013; 118(10) 5018-5028.